Ultrasonic surgical devices driven by piezoelectric tubes

Xuan Li
Centre for Medical & Industrial Ultrasonics, James Watt School of Engineering
University of Glasgow
Glasgow, UK
Xuan.Li@glasgow.ac.uk

Nicola Giuseppe Fenu
Centre for Medical & Industrial Ultrasonics, James Watt School of Engineering
University of Glasgow
Glasgow, UK
Nicola.Fenu@glasgow.ac.uk

Sandy Cochran
Centre for Medical & Industrial Ultrasonics, James Watt School of Engineering
University of Glasgow
Glasgow, UK
Sandy.Cochran@glasgow.ac.uk

Margaret Lucas
Centre for Medical & Industrial Ultrasonics, James Watt School of Engineering
University of Glasgow
Glasgow, UK
Margaret.Lucas@glasgow.ac.uk

***Abstract*—Minimally invasive surgery can potentially benefit from the use of ultrasonic devices through their high precision, low force, and tissue selectivity, thus reducing morbidity, recovery time and cost. To facilitate this, miniature ultrasonic surgical tools are required, integrated with flexible surgical robots to guide them to surgical sites inside the body. This paper presents two novel designs of miniature ultrasonic surgical devices excited by a radially polarized piezoelectric tube. One configuration employs the longitudinal mode of the tube and the other uses the breathing mode in a flextensional configuration, to achieve a longitudinal motion of the blade. Experimental results show that the vibration at the tip of the blade of the cymbal end-cap (flextensional configuration) has developed a 4-6 times higher amplitude with the same excitation than the stepped horn (longitudinal configuration), demonstrating potential for using the breathing mode of the piezoelectric tube.**

Keywords—Piezoelectric tube, miniature ultrasonic surgical device, longitudinal mode, breathing mode, flextensional

I. INTRODUCTION

Ultrasonic surgery, as an alternative to the most commonly used electrosurgery or laser surgery, offers important benefits such as minimal lateral thermal tissue damage, charring, desiccation, or smoke in the surgical region, as well as greater cutting precision near vital structures, excellent haemostasis, and reduced risks of current passage to the patient [1].

Ultrasonically activated scalpels cut tissues with a sharp blade, vibrating at a resonance frequency in the range of 25 to 55 kHz with a displacement amplitude of up to 100 µm and at a power level of tens of watts [2]. For hard tissue cutting, for example Piezosurgery® [3], the ultrasonic surgical devices are operated at a low frequency (between 20 and 35 kHz), with surgical tips exhibiting tissue selectivity [4] and cutting with low force. Soft tissue cutting devices, often referred to as ultrasonic shears, can perform both dissection and vessel sealing, but they require a larger displacement amplitude and normally operate at a frequency around 50 kHz [5], [6]. These devices are widely adopted for laparoscopic surgeries, such as the Harmonic Ace® [7] operating at a 55 kHz resonance frequency.

Despite developments in the ultrasonic surgical device technology, such as employing various new geometries of surgical tips for different procedures [8], and utilizing different surgical tip vibration modes [9], hard tissue and soft tissue cutting devices are all based on the configuration of a tuned Bolted Langevin-style Transducer (BLT) with a horn and a cutting insert. However, to be integrated with flexible surgical robots, for minimally invasive surgery, the size of the ultrasonic surgical device needs to be small. Miniaturising BLTs entails a reduction in both length and diameter, causing resonance frequency to increase and volume of piezoelectric material to decrease, which will greatly affect the achievable displacement amplitude at the surgical tip.

Recently, some alternative configurations have been proposed, such as actuating a cymbal metal end-cap in a flextensional configuration with thickness direction polarised piezoelectric discs [10] or plates [11] using the d_{31} or d_{32} modes. These have demonstrated potential for use in bone cutting devices. This paper investigates a new configuration of miniature ultrasonic surgical devices based on a radially polarised piezoelectric tube. Two devices are created, one using the d_{33} mode of the tube to drive a cymbal-shaped end-cap with surgical tip attached, and the other using the d_{31} mode of the tube to drive a stepped horn with surgical tip attached.

II. ULTRASONIC SURGICAL DEVICES

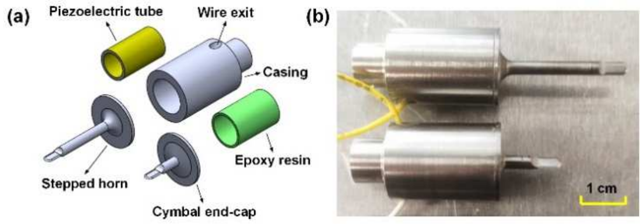

Fig. 1. Ultrasonic surgical devices based on a piezoelectric tube: (a) device components, (b) fabricated utlrasonic surgical devices (top: device excited by the longtudinal mode of the tube with a stepped horn, bottom: device actuated with the breathing mode of the tube with a cymbal end-cap)

The exploded view of the two ultrasonic surgical devices based on a radially polarized piezoelectric tube employing the longitudinal mode and breathing mode with a stepped horn and a cymbal end-cap, and the fabricated devices are presented in Fig. 1.

The piezoelectric tube is a hard PZT piezoceramic (PIC-181, PI Ceramic GmbH, Germany) material, and the dimensions and material properties are presented in TABLE I.

The casing is made from titanium grade 5 alloy, Ti-6Al-4V, with a central hole to accommodate the piezoelectric tube. A recessed cylindrical solid tail mass structure is located at the rear of the casing for external clamping purpose for tissue

The research was supported by an EPSRC Programme Grant (Ultrasurge – Surgery enabled by Ultrasonics, EP/R045291/1)

cutting experiments. Two holes close to the bottom of the central hole allow for electrical wires to exit. A stepped horn and a cymbal end-cap can be attached to the same transducer to achieve the longitudinal mode of the cutting blade at the same resonance frequency, one of which (stepped horn) uses the longitudinal mode excitation of the tube and the other (cymbal end-cap) employs the breathing mode of the tube.

TABLE I. PIC-181 TUBE MATERIAL PROPERTIES

Outer diameter [mm]	10
Inner diameter [mm]	8
Length [mm]	17
Density ρ [kg/m^3]	7850
Relative permittivity ε_{11}^{T}	1224
Relative permittivity ε_{33}^{T}	1135
Piezoelectric charge coefficient d_{31} [m/V]	-1.08×10^{-10}
Piezoelectric charge coefficient d_{33} [m/V]	2.53×10^{-10}
Piezoelectric charge coefficient d_{15} [m/V]	3.89×10^{-10}
Elastic compliance coefficient s_{11}^{E} [m^2/N]	1.175×10^{-11}
Elastic compliance coefficient s_{33}^{E} [m^2/N]	1.411×10^{-11}
Poisson's ratio ν	0.35
Q	2200
Curie temperature [°C]	330

TABLE II. EPOXY MATERIAL PROPERTIES

Material	Silver conductive epoxy	Epoxy resin
Density [kg/m^3]	2600	1060
Hardness [Shore-D]	70	75
Flexural strength [MPa]	17	57
Shear strength [MPa]	8	16.5
Tensile strength [MPa]	13	-
Compressive strength [MPa]	39	-
Temperature range [°C]	-55 to 150	-40 to 90
Volume resistivity [Ω.cm]	0.007	$>1 \times 10^{13}$

TABLE III. TRANSDUCER MATERIAL PROPERTIES AND DIMENSIONS

Material	Titanium grade 5 Ti-6Al-4V
Density [kg/m^3]	4430
Young's modulus [GPa]	109
Poisson's ratio ν	0.313
Acoustic impedance [$\text{Pa.s/m} \times 10^6$]	27.32
Component	Casing
Length [mm]	31
Outer diameter [mm]	17
Inner diameter [mm]	11.5
Central Hole depth [mm]	17
Tail mass diameter [mm]	10
Tail mass length [mm]	8
Component	Stepped horn
Length [mm]	29
Cap diameter [mm]	17
Cap thickness [mm]	1
Rod diameter [mm]	3
Blade thickness [mm]	0.5
Fillet radius [mm]	3
Component	Cymbal end-cap
Length [mm]	14.3
Cap diameter [mm]	17
Cap thickness [mm]	0.9
Cavity based diameter [mm]	11.5
Cavity apex diameter [mm]	3
Cavity height [mm]	0.9
Rod diameter [mm]	3
Blade thickness [mm]	0.5

During fabrication, two electrical wires were attached to the inner and outer circumferential surfaces of the piezoelectric tube using a silver conductive epoxy (8331-14G, MG Chemicals Ltd, Canada) instead of soldering, to avoid the risk of depolarisation of the piezoelectric material. Thereafter, insulating epoxy resin (Eccobond, Ellsworth Adhesives Ltd, UK) was prepared with a mixing ratio 1:1 (rigid formula) and filled the gap of the central hole of the casing and outer circumferential surface of the tube to form the bonding layer. The stepped horn and cymbal end-cap were then attached to the transducer with the same epoxy resin. Epoxies were cured for 48 hours and their material properties are shown in TABLE II. Material properties and dimensions of the casing, stepped horn and cymbal end-cap are shown in TABLE III.

The piezoelectric tube, ultrasonic transducer and both surgical devices were all characterised using electrical impedance analysis and experimental modal analysis. Further, displacement amplitudes at the blade of the surgical devices were recorded with harmonic response analysis.

III. RESULTS AND DICUSSION

A. Impedance

Impedances of the tube, transducer and surgical devices were measured using an impedance analyser (Agilent 4294A, Agilent Technologies, CA, USA). A swept signal of 1 V peak-to-peak over a bandwidth of the frequency range of interest was applied, and the impedance spectrum was measured. The effective coupling coefficient, k_{eff}, was calculated from the impedance measurements from equation (1) [12]:

$$k_{eff}^2 = \frac{f_a^2 - f_r^2}{f_a^2} \quad (1)$$

f_r is the resonance frequency and f_a is the anti-resonance frequency.

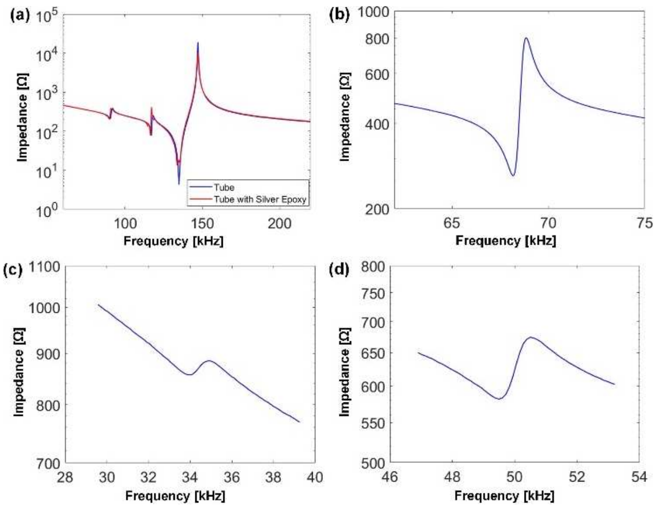

Fig. 2. Electrical impedance measurements: (a) piezoelectric tube, (b) ultrasonic transducer, (c) surgical device with stepped horn, (d) surgical device with cymbal end-cap

From the measured impedance spectrum of the piezoelectric tube (Fig. 2 (a)), three peaks were identified in a frequency range up to 200 kHz, representing the longitudinal mode, breathing mode and expanding mode (not used), respectively, confirmed from the modal analysis results (next section). The silver conductive epoxy has influenced the resonance frequencies and impedance values of the three peaks (See TABLE IV). More importantly, the coupling coefficient k_{eff} has decreased by 30-40%, which is going to affect the achievable vibration displacement of the piezoelectric tube once it is embedded in the metal casing. The fabricated transducer (without horn or end-cap attached) shows a resonance frequency of 68 kHz in the longitudinal mode, mainly due to the effects of the added mass of the casing and epoxy resin on the longitudinal mode frequency (90 kHz) of the piezoelectric tube.

The impedance spectrum of the device excited by the longitudinal mode of the piezoelectric tube (Fig. 2 (c)) presents an unusual characteristic, with similar impedance values at resonance and anti-resonance, possibly due to the radial motion of the tube being constrained by the epoxy and metal casing when excited in the longitudinal mode. As a comparison, the impedance curve of the device employing the breathing mode of the tube (Fig. 2 (d)) exhibits a less damped response.

TABLE IV. ELECTRICAL CHARACTERISTICS OF THE SURGICAL TOOLS

Part	Tube	Tube with silver epoxy
f_r – longitudinal [Hz]	90238	90238
f_a – longitudinal [Hz]	92075	90850
K_{eff} – longitudinal	0.199	0.116
Z – longitudinal [Ω]	210	200
f_r – breathing [Hz]	117188	116575
f_a – breathing [Hz]	118413	117188
k_{eff} – breathing	0.144	0.102
|Z| – breathing [Ω]	78	77

Assembly	Transducer	Stepped horn device	Cymbal end-cap device
f_r [Hz]	68158	33963	49488
f_a [Hz]	68840	34863	50500
k_{eff}	0.140	0.226	0.199
|Z| [Ω]	261	857	582

B. *Mode shape*

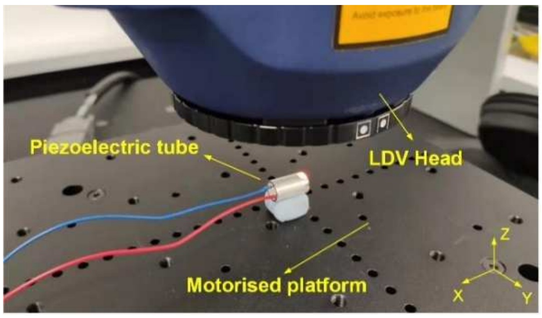

Fig. 3. Experimental modal analysis of the piezoelectric tube using 3D laser vibrometry (Polytec MSA-100)

EMA was performed by measuring the frequency response functions (FRFs) from a grid of vibration response measurement points along an axial line on the surface of the piezoelectric tube, transducer and the two surgical devices, from which the modal parameters (frequency, damping, and mode shape) were extracted, using a 3D laser vibrometry (MSA-100-3D, Polytec GmbH, Germany). Fig. 3 illustrates the EMA set-up for the piezoelectric tube. A white noise excitation of 5 V was generated by signal generator and was supplied to the piezoelectric material. The 3D laser Doppler vibrometer measured three orthogonal components of the vibrational velocities from the grid points. Data acquisition and processing software (PSV, Polytec GmbH, Germany) was used to calculate the FRFs from the excitation and response signals and then to apply curve-fitting routines to extract the mode shape magnitude and phase data.

The predicted vibration mode shapes of the piezoelectric tube using finite element analysis (FEA) (Abaqus-Simulia, Dassault Systèmes, France) and the measured mode shapes are presented in Fig. 4.

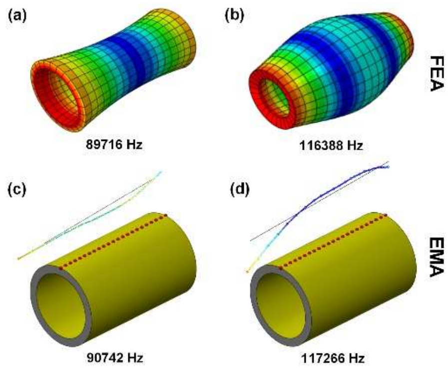

Fig. 4. Predicted and measured vibraiton mode shapes of the piezoelectric tube: (a) predicted longitudinal mode, (b) predicted breathing mode, (c) measured longitudinal mode, (d) measured breathing mode. Red dots are measurement points on the surface of the piezoelectric tube, and solid black line represents the undeformed shape

The FEA and EMA results show an agreement with respect to the resonance frequencies. The silver conductive epoxy has slightly influenced the deformation of the piezoelectric tube, but the location of the maximal contraction of the tube in the longitudinal mode and displacement nodes of the breathing mode are in an agreement.

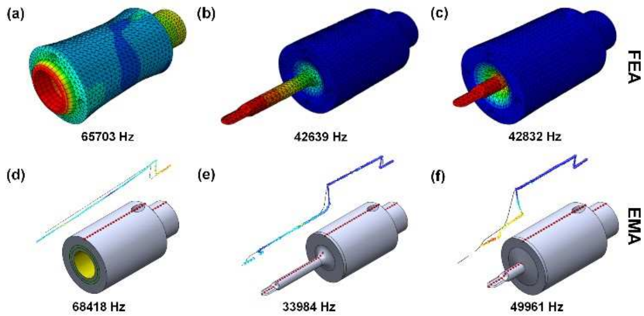

Fig. 5. Predicted and measured vibration mode shapes of the ultrasonic transducer and surgical devices: (a) – (c) predicted longitudinal modes of the transducer, stepped horn device and cymbal end-cap device, (d) – (f) measured longitudinal modes of the transducer, stepped horn device and cymbal end-cap device. Red dots stand for the measurement points, and solid black line represents the undeformed shape

The ultrasonic transducer shows a good match of the resonance frequency and longitudinal mode shape between FEA and EMA (Fig. 5 (a) and (d). Two ultrasonic surgical devices employing the longitudinal mode and breathing mode of the piezoelectric tube were designed to resonate at 43 kHz, and the longitudinal mode shapes from FEA are shown in Fig. 5 (b) and (c).

However, the two fabricated surgical devices exhibit large differences in the longitudinal resonance frequencies from FEA predictions (of 7~8 kHz). It is known that resonance frequency is extremely sensitive to the thickness of the cymbal end-cap and height of the apex, therefore manufacturing tolerances may be contributing to the difference in resonance frequency. However, it is expected that a major factor is poor control of the application of the epoxy resin during device fabrication, where there was leakage into the centre of the tube and the end-cap once it was attached [13]. This will also deteriorate the dynamic performance of the piezoelectric tube, seen as a significant reduction in k_{eff} in TABLE IV. For the stepped horn device, the radial movement of the tube (Fig. 3 (a) and (c)) has likely been constrained by the surrounding epoxy and metal casing in the longitudinal mode, which in turn significantly affects the longitudinal motion of the tube and the device, resulting in the lower vibration displacement amplitude of the blade compared with the device with a cymbal end-cap.

C. Vibration response

The devices were excited via a frequency sweep through a range from below to above resonance, using a burst sine signal generated from a signal generator (Agilent 33210A, Agilent Technologies, USA) and amplified by a power amplifier (HFVA-62, Foneng Technology Industry Co., China). The longitudinal vibration was measured using a 1D laser Doppler vibrometer (OFV 303, Polytec GmbH, Germany) at the tip of the blade. To minimise heating effects, each burst sine signal had a fixed 6000 oscillation cycles, and a 2 s time interval between successive bursts. Vibration response data were captured with a 5 Hz resolution, and the applied voltage was stepped from 1, then 10 to 100 V (rms) in increments of 10 V.

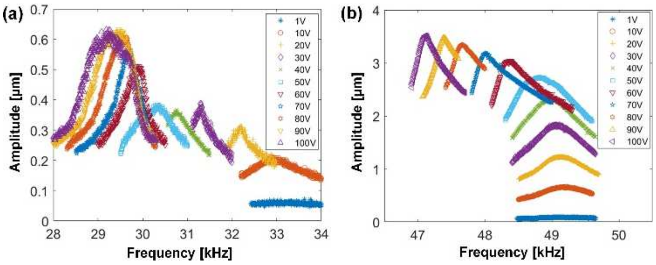

Fig. 6. Vibration displacement amplitude response at the tips of the blades of the ultrasonic surgical devices: (a) stepped horn, (b) cymbal end-cap

Fig. 6 shows the vibration response at the tip of the blade of the two ultrasonic surgical tools.

A less than 400 Hz resonance frequency decrease was observed for a voltage up to 50 V for the cymbal end-cap device [14], followed by a drastic change of a 2 kHz reduction at 100 V, indicating a softening of the epoxy resin. Maximal displacement amplitude at the blade tip is 3.5 µm. For the stepped horn device, a more than 4 kHz frequency reduction was observed through the excitation level range of 1 to 100 V. Also, the damping increases, again indicative of a softening epoxy layer and consequent poorer performance of the longitudinal mode of the tube. The developed amplitude is very low for the stepped horn device.

IV. Conclusion and Future Work

This research has proposed two novel designs of miniature ultrasonic surgical devices based on the use of a piezoelectric tube, employing the longitudinal mode and breathing mode and incorporating a stepped horn and a cymbal end-cap to achieve the longitudinal motion of the blade.

Experimental results show that the epoxy has caused a reduced performance of the piezoelectric tube by decreasing the coupling coefficient k_{eff}. The epoxy has also resulted in a major mismatch of resonance frequency of both surgical devices between FEA and measurements. The displacement amplitude at the tip of the blade of the configuration employing the longitudinal mode (d_{31}) excitation of the piezoelectric tube with a stepped horn has presented only 0.6 µm. This is due to the radial movement of the tube in the longitudinal mode being highly constrained by the fabrication using epoxy and casing. As a comparison, for the device excited by the tube's breathing mode (d_{33}) and a cymbal end-cap, a maximal 3.5 µm is developed at the blade tip. This configuration transforms the radial vibration excitation into a longitudinal motion of the blade by employing the flextensional mechanism. Future work will be focused on the optimization of the geometry of the cymbal end-cap to decrease its stiffness and reduce the resonance frequency of the device in order to increase the displacement amplitude of the blade.

References

[1] J. Clymer, D. Broughton, A. Welling, E. Monroe, K. Pirozzi, and J. Schulte, "Tissue effects in vessel sealing and transection from an ultrasonic device with more intelligent control of energy delivery," *Medical Devices: Evidence and Research*, Vol. 6, pp. 151–154, 2013.

[2] M. Lucas, A. Gachagan, and A. Cardoni, "Research applications and opportunities in power ultrasonics," *Journal of Mechanical Engineering Science: Part C*, vol. 223, pp. 2949–2965, 2009.

[3] M. Labanca, F. Azzola, R. Vinci, and L. F. Rodella, "Piezoelectric surgery: Twenty years of use," *British Journal of Oral Maxillofacial Surgery*, vol. 46, no. 4, pp. 265–269, 2008.

[4] G. Leonardo Magrin, E. Alberto Sigua-Rodriguez, D. Rangel Goulart, and L. Asprino, "Piezosurgery in Bone Augmentation Procedures Previous to Dental Implant Surgery: A Review of the Literature," *The Open Dentistry Journal*, vol. 9, no. 1, pp. 426–430, 2015.

[5] P. Leclercq, C. Zenati, S. Amr, and D. M. Dohan, "Ultrasonic Bone Cut Part 1: State-of-the-Art Technologies and Common Applications," *Journal of Oral and Maxillofacial Surgery*, vol. 66, no. 1, pp. 177–182, 2008.

[6] B. J. O'Daly, E. Morris, G. P. Gavin, J. M. O'Byrne, and G. B. McGuinness, "High-power low-frequency ultrasound: A review of tissue dissection and ablation in medicine and surgery," *Journal of Materials Processing Technology*, vol. 200, no. 1–3, pp. 38–58, 2008.

[7] D. G. Nicastri, M. Wu, J. Yun, and S. J. Swanson, "Evaluation of efficacy of an ultrasonic scalpel for pulmonary vascular ligation in an animal model," *The Journal of Thoracic and Cardiovascular Surgery*, vol. 134, no. 1, pp. 160–164, 2007.

[8] G. Plotino, C. H. Pameijer, N. Maria Grande, and F. Somma, "Ultrasonics in Endodontics: A Review of the Literature," *Journal of Endodontics*, vol. 33, no. 2. pp. 81–95, 2007.

[9] S. C. Lea, B. Felver, G. Landini, and A. D. Walmsley, "Three-dimensional analyses of ultrasonic scaler oscillations," *Journal of Clinical Periodontology*, vol. 36, no. 1, pp. 44–50, 2009.

[10] F. Bejarano, A. Feeney, R. Wallace, H. Simpson, and M. Lucas, "An ultrasonic orthopaedic surgical device based on a cymbal transducer," *Ultrasonics*, vol. 72, pp. 24–33, 2016.

[11] L. Luo, Y. Tang, F. Wang, C. He, and H. Luo, "Displacement amplification and electric characteristics of modified rectangular cymbal transducers using electroactive materials," *Solid State Communications*, vol. 143, no. 6–7, pp. 321–325, 2007.

[12] A. Caronti, R. Carotenuto, and M. Pappalardo, "Electromechanical coupling factor of capacitive micromachined ultrasonic transducers," *The Journal of the Acoustical Society of America*, vol. 113, no. 1, pp. 279–288, 2003.

[13] J. F. Fernández, A. Dogan, J. T. Fielding, K. Uchino, and R. E. Newnham, "Tailoring the performance of ceramic-metal piezocomposite actuators, 'cymbals,'" *Sensors and Actuators A*, vol. 65, no. 2–3, pp. 228–237, 1998.

[14] A. Mathieson, A. Cardoni, N. Cerisola, and M. Lucas, "The influence of piezoceramic stack location on nonlinear behavior of langevin transducers," *IEEE Transactions on Ultrasonics, Ferroelectrics and Frequency Control*, vol. 60, no. 6, pp. 1126–1133, 2013.